J Therm Anal Calorim (2009) 97:911–915
DOI 10.1007/s10973-009-0094-4

Experimental and theoretical cooling velocity profile inside laser welded metals using keyhole approximation and Boubaker polynomials expansion

Asma Belhadj · Jamel Bessrour · Mahmoud Bouhafs · Laurent Barrallier

Received: 28 October 2008 / Accepted: 6 January 2009 / Published online: 29 August 2009

Abstract In this paper we are concerned with the t-dependent cooling velocity during laser welding sequences. The temperature profile has been yielded by using keyhole approximation for the melted zone and solving the heat transfer equation. A polynomial expansion has been adopted as a guide to determining the cooling velocity during welding cut-off stage. A thorough comparison with experimental results and recently published profiles has been carried out.

Keywords Laser welding · Keyhole model · Cooling velocity · Boubaker polynomials · Temperature profiling

PACS 02.00.00 · 02.30.Jr · 02.60.Lj

A. Belhadj (✉)
U.R. MA2I - L. MECASURF, ENIT - Art et Métiers ParisTech, Aix-en-Provence, France
e-mail: assma_belhadj@yahoo.fr

J. Bessrour · M. Bouhafs
U.R. MA2I, ENIT, Tunis, Tunisia
e-mail: jamel.bessrour@enit.rnu.tn

M. Bouhafs
e-mail: mahmoud.bouhafs@enit.rnu.tn

L. Barrallier
L. MECASURF, Art et Métiers ParisTech, Aix-en-Provence, France
e-mail: laurent.barrallier@ensam.eu

Introduction

In the last decades, a huge increase in the need for high power lasers for precision welding has been noticed. Parallel to this trend, laser welding computing numerical techniques have improved to the point where numerical modelling [1–6] began more and more accepted as a guide to prediction of weld geometries and temperature profiling.

The laser welding keyhole (Fig. 1) model was proposed in the earliest studies as an alternative to both Gaussian and double ellipsoidal (DE) models. In the end of the last decade, two relevant models were consecutively proposed and discussed by Singh and Narayan [1] and Anisimov et al. [2]. The latter model was more realistic, since it did not adopt the assumption of isothermal expansion inside the keyhole.

In this study, we tried to set a cylindrical model as a guide to solve the heat equation inside the heated keyhole and evaluate the cooling velocity in the relaxation phase.

Keyhole approximation model

In this section we try to describe the keyhole and its formation relevant steps (Fig. 2).

Our keyhole approximation model (Fig. 3) is based on the following assumptions:

- The keyhole vertical edges temperature is equal to the boiling point of the material.
- The heat transfer along directions perpendicular to the incident laser beam is invariant under cylindrical symmetry.
- The heat source is assumed to be Gaussian and centred along the keyhole axis.

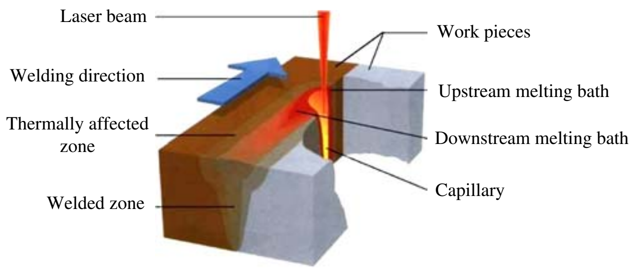

Fig. 1 Keyhole formation scheme

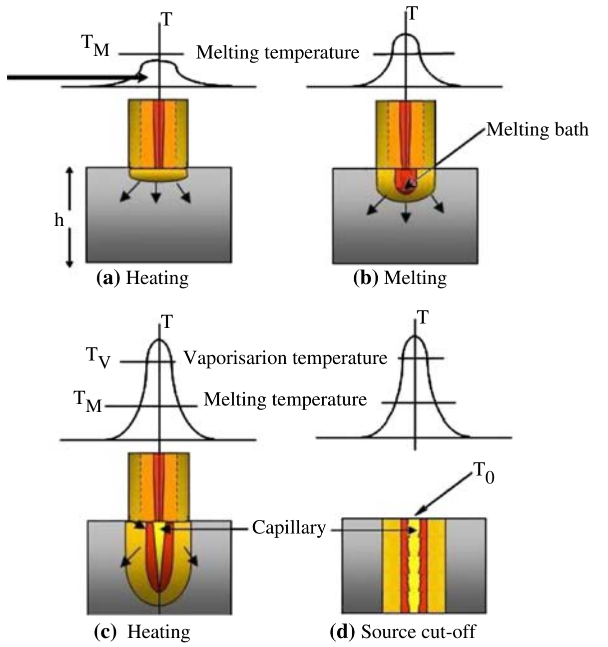

Fig. 2 Steps and mechanism of keyhole formation

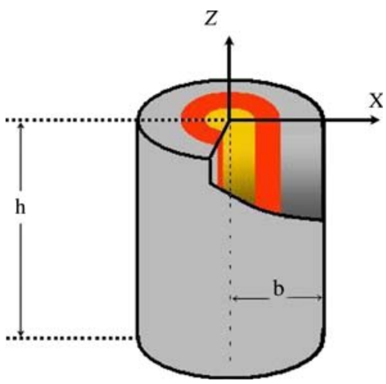

Fig. 3 Keyhole geometrical representation

– The exciting beam thermal and optical profiles are coherent.

These assumptions are justified on the grounds that keyhole both vertical and radial extents h and b, respectively (Fig. 3), are small when compared to bulk ones.

The starting point of the modelling procedure is identified to the source cut-off date (Fig. 2d).

Theoretical investigations

Source term

The first step in the theoretical investigation consists of defining the power Q_v per unit volume absorbed by the keyhole:

$$Q_v = \frac{P_{ak}}{V_{keyhole}} = \frac{4P_{ak}}{h\pi b^2} \tag{1}$$

where P_{ak} is the total power absorbed by the keyhole volume.

This volumetric source term will be useful for determining the maximal central temperature T_0.

Heat equation

In respect to the assumptions expressed in the section "Keyhole approximation model", the main heat equation inside the keyhole is:

$$\begin{cases} \dfrac{\partial T(x,t)}{\partial t} = \dfrac{1}{D}\dfrac{\partial^2 T(x,t)}{\partial x^2}, & t > 0;\ |x| < b \\ T(x,t)|_{t=0} = T_0 \times e^{-\frac{x^2}{2b^2}}; & T(x,t)|_{t\to\infty} = T_\infty \end{cases} \tag{2}$$

where T_∞ is the room temperature.

$T(x,t)$ is first expressed as an infinite sum of the B. polynomials [7–11], whose expression fits boundary condition.

$$T(x,t) = T_0 \times e^{-\frac{x^2}{2b^2}} \times \frac{1}{2N_0}\sum_{n=1}^{N_0} \xi_n \cdot B_{4n}\left(t\frac{\alpha_n}{t_m}\right) \tag{3}$$

where α_n are the minimal positive roots of the Boubaker 4n-order polynomials B_{4n} [9–11], r_m is the maximum sheet radial range (where the temperature is supposed to be room one), N_0 is an even given integer, T_0 is the maximal central temperature and ξ_n are coefficients to be found.

Equation (2) is then altered to:

$$T_0 \times e^{-\frac{x^2}{2b^2}} \times \frac{1}{2N_0}\sum_{n=1}^{N_0} \xi_n \frac{\alpha_n}{t_m} B'_{4n}\left(t\frac{\alpha_n}{t_m}\right) = \frac{1}{D} T_0 \times e^{-\frac{x^2}{2b^2}}\left(\frac{x^2}{b^4} - \frac{x}{b^2}\right) \times \frac{1}{2N_0}\sum_{n=1}^{N_0} \xi_n \cdot B_{4n}\left(t\frac{\alpha_n}{t_m}\right) \tag{4}$$

which gives:

$$\sum_{n=1}^{N_0} \xi_n \frac{\alpha_n}{t_m} B'_{4n}\left(t\frac{\alpha_n}{t_m}\right) = \frac{1}{D}\left(\frac{x^2}{b^4} - \frac{x}{b^2}\right)\sum_{n=1}^{N_0} \xi_n \cdot B_{4n}\left(t\frac{\alpha_n}{t_m}\right) \tag{5}$$

and the system:

$$\begin{cases} \sum_{n=1}^{N_0} \xi_n = -N_0 \\ \sum_{n=1}^{N_0} \xi_n \frac{\alpha_n}{t_m} B'_{4n}(\alpha_n) = 0 \end{cases} \quad (6)$$

Thanks to the Boubaker polynomials properties:

$$\begin{cases} B_{4(q+1)}(X) = \left(X^4 - 4X^2 + 2\right) \times B_{4(q)}(X) - B_{4(q-1)}(X) \\ B_{4q}^2(X) - B_{4(q-1)}(X) \times B_{4(q+1)}(X) = X^2\left(X^2-1\right)^2\left(3X^2+4\right) \\ B_{4(q)}\left(\alpha_q\right) = 0. \end{cases} \quad (7)$$

which gives:

$$\begin{cases} B_{4(q+1)}\left(\alpha_q\right) = -B_{4(q-1)}\left(\alpha_q\right) \\ -B_{4(q-1)}\left(\alpha_q\right) \times B_{4(q+1)}\left(\alpha_q\right) = X^2\left(X^2-1\right)^2\left(3X^2+4\right)\Big|_{X=\alpha_q} \\ B'_{4(q)}\left(\alpha_q\right) \approx \dfrac{B_{4(q+1)}\left(\alpha_q\right) - B_{4(q-1)}\left(\alpha_q\right)}{2\alpha_q} \end{cases} \quad (8)$$

and

$$B'_{4(q)}\left(\alpha_q\right) = \frac{2\alpha_q^2\left(\alpha_q^2-1\right)^2\left(3\alpha_q^2+4\right)}{2\alpha_q} \quad (9)$$

the system (6) is reduced to:

$$\begin{cases} \sum_{n=1}^{N_0} \xi_n = -N_0 \\ \sum_{n=1}^{N_0} \xi_n \times u_n = 0; \quad \text{with } u_n = \left[\alpha_n^2(\alpha_n^2-1)^2(3\alpha_n^2+4)\right] \end{cases} \quad (10)$$

A solution to the system (10) is:

$$\xi_n = -N_0 \frac{\theta(n) \times u_{(N_0-n+1)}}{\left(\sum_{n=1}^{N_0} \theta(n) \times u_{(N_0-n+1)}\right)}; \quad \text{with } \theta(n) = \begin{cases} -1 \text{ if } n < \dfrac{N_0}{2} \\ 1 \text{ if } n > \dfrac{N_0}{2} \end{cases} \quad (11)$$

The correspondent calculated parameters are gathered in Table 1.

Determination of T_0

T_0 is obtained by analogy with Coulomb approximation [12, 13]:

Table 1 Parameters values

$n = 4q$	α_n	u_n	$\theta(n) \times u_{(N_0-n+1)}$	ξ_n
1	1.1894	2.00542	−0.03973	0.1090
2	0.5078	0.67795	−0.05730	0.4912
3	0.3114	0.33931	−0.07947	0.2188
4	0.2236	0.18726	−0.11672	0.3201
5	0.1742	0.11672	0.18726	−0.5116
6	0.1428	0.07947	0.33931	−0.930
7	0.1208	0.0573	0.67795	−1.8595
8	0.1003	0.03973	2.00542	−5.0050
$N_0 = 8$	$\sum_{n=1}^{N_0} \theta(n) \times u_{(N_0-n+1)} = 2.91672$			$\sum_{n=1}^{N_0} \xi_n = -N_0$

When a b-radius cylindrical material with thermal conductivity k, receives a uniformly distributed power P (figure), its surface constant temperature rise is expressed by (12):

$$T_0 = \frac{P \;\, 1}{2\pi k b} \quad (12)$$

Our studied model differs from this general approach by non uniformity of the heat distribution. By analogy, an approximation of maximum central temperature can be obtained by replacing term b in expression (12) by an equivalent radius value $\hat{b}$ defined as an arithmetical mean of radii weighted by elementary incident intensity on an elementary r-associated volume dV, which is an r-radius hollow cylinder of thickness dr and height h:

$$\hat{b} = \frac{\int_0^{+\infty} e^{-\frac{x^2}{2b^2}} 2\pi h x \mathrm{d}x}{\int_0^{+\infty} e^{-\frac{x^2}{2b^2}} 2\pi x \mathrm{d}x} = \frac{2b}{\sqrt{\pi}} \quad (13)$$

The source term is also approximated as a Gaussian distribution:

$$P = \int_{-h}^{0} \left(\int_0^{+\infty} Q_{\mathrm{v}} \times e^{-\frac{x^2}{2b^2}} 2\pi x \mathrm{d}x \right) \mathrm{d}z = \int_{-h}^{0} \int_0^{+\infty} \frac{4P_{\mathrm{ak}}}{h\pi b^2} \times e^{-\frac{x^2}{2b^2}} 2\pi x \mathrm{d}x \mathrm{d}z = \frac{8P_{\mathrm{ak}}}{\sqrt{\pi}} \quad (14)$$

We obtain finally:

$$T_0 = \frac{2P_{\mathrm{ak}}}{\pi k b} = \frac{hbQ_{\mathrm{v}}}{2k} \quad (15)$$

The temperature profile is deduced from (Eqs. 3, 11, 15) and the values shown in Table 1.

Experiment

Experimental setup

The laser welding was carried out using a ROFIN DC030 CO_2 laser source setup (Fig. 4). The produced beam is deviated toward the targeted zone by copper mirrors.

The work pieces were two 3 mm thick Magnesium AM60 sheets. The laser power was 3 kW in TEM_{01} mode. The welding speed was set to 4.2 m min^{-1} under a Helium flow of 40 L min^{-1}.

Measurements $T = f(t)$ mounting

Temperature measurements were carried out using detachable thermocouples linked to data-processing unit via NI 9012 connectable modules (Fig. 5).

Results and discussion

The obtained temperature evolution is presented in (Fig. 6) along with theoretical results detailed in the section "Theoretical investigations".

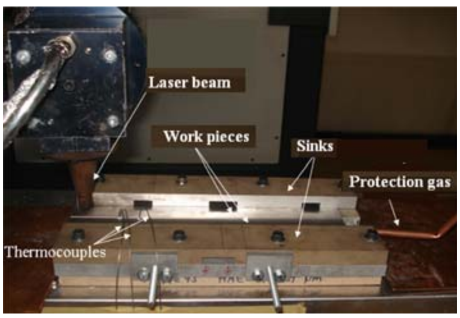

Fig. 4 Experimental setup

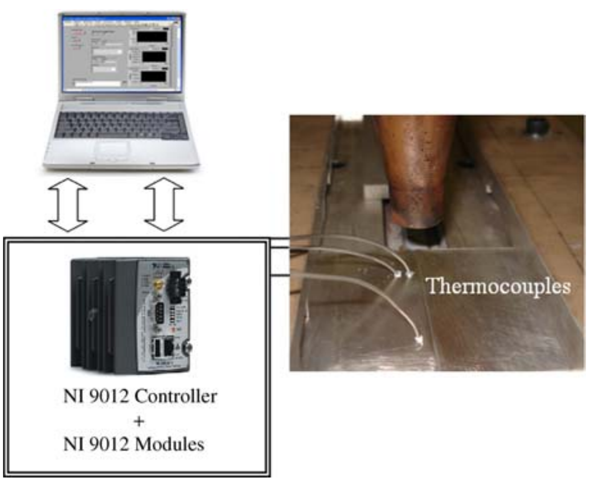

Fig. 5 Temperature measurement mounting

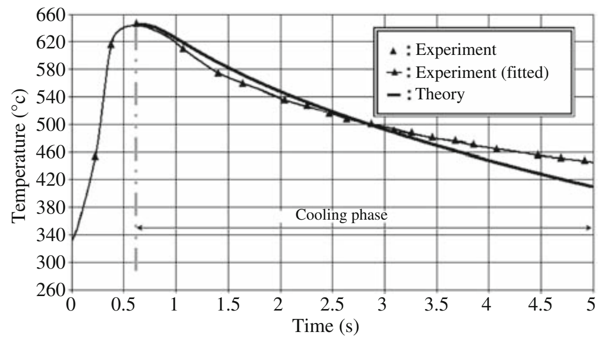

Fig. 6 Temperature evolution (theory and experiment)

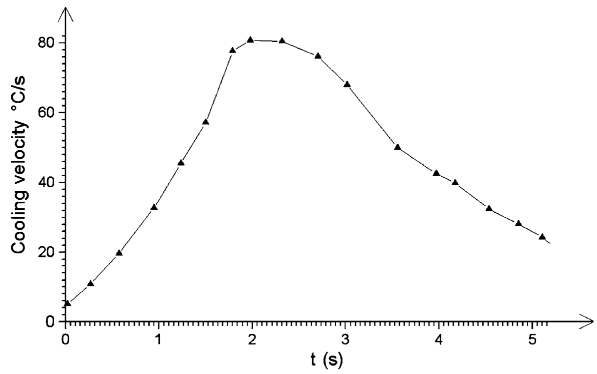

Fig. 7 The cooling velocity profile

It is known that a good knowledge of the cooling velocity profile is necessary for predicting and monitoring many interesting items like initial solidification uniformity, slab solidification structure, and metal purity. In this context, the cooling velocity profile (Fig. 7) was derived from the results shown in (Fig. 6, cooling phase). It is noted that using DERIVE_6 software, the time ($t = 0$) corresponds to the cooling phase starting date ($\approx$0.6 s in Fig. 6).

The shape of this profile (Fig. 7) is in concordance with the profiles presented by Paul and Debroy [14], Andreassen et al. [15] and °Belcher [16]. The velocity range (0–82 °C s^{-1}) is also agreeing with the values published by Santos et al. [17] and more recently by Mughal et al. [18].

Conclusions

A theoretical–experimental model of heat transfer inside a cylindrical keyhole laser welding [19–28] was presented. The yielded temperature evolution was compared to both experimental results and recently published results [14–32]. The model was adapted in order to evaluate the cooling velocity.

Actually, we are trying to exploit the present model, by implementing real-time velocity measurements, in order to prove that the cooling velocity can be reduced by the presence of appropriate alloying elements. This feature is very interesting since it is an issue for hardening with mild quenching.

Acknowledgements The authors would like to acknowledge help and assistance from Associate Prof. Dr K. Boubaker from University of Tunis (Tunisia).

References

1. Singh RK, Narayan J. Pulsed-laser evaporation technique for deposition of thin films: physics and theoretical model. Phys Rev B. 1990;41:8843–59.
2. Anisimov SI, Luk'yanchuk BS, Luches A. An analytical model for three-dimensional laser plume expansion into vacuum in hydrodynamic regime. Appl Surf Sci. 1996;96–98:24–32.
3. Koopman DW. Langmuir probe and microwave measurements of streaming plasmas generated by focused laser pulses. Phys Fluids. 1971;14:1707–16.
4. Toftmann B, Schou J, Hansen TN, Lunney JG. Evolution of the plasma parameters in the expanding laser ablation plume of silver. Phys Rev Lett. 2000;84:3998–4001.
5. Weaver I, Martin GW, Graham WG, Morrow T, Lewis CLS. The Langmuir probe as a diagnostic of the electron component within low temperature laser ablated plasma plumes. Rev Sci Instrum. 1999;70:1801–5.
6. Doggett B, Budtz-Joergensen C, Lunney JG, Sheerin P, Turner MM. Behaviour of a planar Langmuir probe in a laser ablation plasma. Appl Surf Sci. 2005;247:134–8.
7. Chaouachi A, Boubaker K, Amlouk M, Bouzouita H. Enhancement of pyrolysis spray disposal performance using thermal time-response to precursor uniform deposition. Eur Phys J Appl Phys. 2007;37:105–9.
8. Ghanouchi J, Labiadh H, Boubaker K. An attempt to solve the heat transfer equation in a model of pyrolysis spray using 4q-order Boubaker polynomials. Int J Heat Technol. 2008;26:49–53.
9. Awojoyogbe OB, Boubaker K. A solution to Bloch NMR flow equations for the analysis of homodynamic functions of blood flow system using m-Boubaker polynomials. Curr Appl Phys. 2009;9:278–83.
10. Boubaker K. On modified Boubaker polynomials: some differential and analytical properties of the new polynomials issued from an attempt for solving bi-varied heat equation. Trends Appl Sci Res. 2007;2:540–4.
11. Labiadh H. A Sturm-Liouville shaped characteristic differential equation as a guide to establish a quasi-polynomial expression to the Boubaker polynomials. J Differ Equ Control Process. 2007;2:117–33.
12. Gallusser R, Dressler K. Application of the coulomb approximation to the Rydberg transitions of the NO molecule. Z Angew Math Phys. 1971;22:792–4.
13. Armstrong BH, Purdum KL. Extended use of the Coulomb approximation: mean powers of r, a sum rule, and improved transition integrals. Phys Rev. 1966;150:51–8.
14. Paul A, Debroy T. Free surface flow and heat transfer in conduction mode laser welding. Metall Mater Trans B. 1988;19:851–8.
15. Andreassen E, Myhre OJ, Oldervoll F, Hinrichsen EL, Grøstad K, Braathen MD. Nonuniform cooling in multifilament melt spinning of polypropylene fibers: cooling air speed limits and fiber-to-fiber variations. J Appl Polym Sci. 1995;58:1619–32.
16. Belcher SL. Practical guide to injection blow molding. Boca Raton, FL: CRC Press; 2007. ISBN 0824757912, 9780824757915.
17. Santos CAC, Quaresma JNN, Lima JA. Convective heat transfer in ducts: the integral transform approach. Brazil: E-papers Servicos Editoriais Ltd; 2001. ISBN 8587922238, 9788587922236.
18. Mughal MP, Fawad H, Mufti R. Finite element prediction of thermal stresses and deformations in layered manufacturing of metallic parts. Acta Mech. 2006;183:61–79.
19. Dowden J, Postacioglu N, Davis M, Kapadia P. A keyhole model in penetration welding with a laser. J Phys D Appl Phys. 1987;20:36–44.
20. Semak VV, Bragg WD, Damkroger B, Kempka S. Transient model for the keyhole during laser welding. J Phys D Appl Phys. 1999;32:61–4.
21. Ki H, Mazumder J, Mohanty PS. Modeling of laser keyhole welding: Part II: simulation of keyhole evolution, velocity, temperature profile, and experimental verification. Metall Mater Trans A. 2002;33:1831–42.
22. Rai R, Kelly SM, Martukanitz RP, DebRoy T. A convective heat-transfer model for partial and full penetration keyhole mode laser welding of a structural steel. Metall Mater Trans A. 2008;39:98–112.
23. Al-Kazzaz H, Medraj M, Caoand X, Jahazi M. Nd:YAG laser welding of aerospace grade ZE41A magnesium alloy: modeling and experimental investigations. Mater Chem Phys. 2008;109:61–76.
24. Kaplan A. A model of deep penetration laser welding based on calculation of the keyhole profile. J Phys D Appl Phys. 1994;27:1805–14.
25. Lampa C, Kaplan AFH, Powell J, Magnusson C. An analytical thermodynamic model of laser welding. J Phys D Appl Phys. 1997;30:1293–9.
26. Jin X, Li L, Zhang Y. A study on fresnel absorption and reflections in the keyhole in deep penetration laser welding. J Phys D Appl Phys. 2002;35:2304–10.
27. Solana P, Negro G. A study of the effect of multiple reflections on the shape of the keyhole of the keyhole in the laser processing of materials. J Phys D Appl Phys. 1997;30:3216–22.
28. Wu CS, Wang HG, Zhang YM. A new heat source model for keyhole plasma arc welding in FEM analysis of the temperature profile. Weld J. 2006;85:284–9.
29. Puchert R, Menzel U, Bärwolff A, Voß M, Lier Ch. Influence of heat source distributions in GaAs/GaAlAs quantum-well high-power laser arrays on temperature profile and thermal resistance. J Therm Anal Calorim. 1997;48:1273–82.
30. Hakvoort G, Hol CM. DSC calibration during cooling. J Therm Anal Calorim. 1999;56:717–22.
31. Holender J, Solstroktys J, Kozubski R. Numerical method of non-isothermal curve analysis by means of electrical resistance measurement during cooling. J Therm Anal Calorim. 1988;33:223–8.
32. Hidvégi É, Csetényi EK, Keébe Gy. The effects of concentration and heating or cooling rate on the DTA curves of Al-Ce alloys. J Therm Anal Calorim. 1977;11:221–9.